Supplementary Table S1: Primers list.

Species	Gene Name	Forward primer (5'-3')	Reverse primer (5'-3')	Purpose
Human	IL-17	AACCGATCCACCTCACCTTG	TCTCTTGCTGGATGGGGACA	qPCR
Human	IL-4	TCTTCCTGCTAGCATGTGCC	TGTTACGGTCAACTCGGTGC	qPCR
Human	IFN-γ	ATGGTTGTCCTGCCTGCAAT	CTTGCTTAGGTTGGCTGCCT	qPCR
Human	IL-23	CCAGCTTCATGCCTCCCTAC	TCTGAGTGCCATCCTTGAGC	qPCR
Human	IL-10	ACATCAAGGCGCATGTGAAC	TAGAGTCGCCACCCTGATGT	qPCR
Human	HDAC-1	CACCCGGAGGAAAGTCTGTTA	TCTTCCAGGCCGTCACCAT	qPCR
Human	HDAC-2	ATTACTGATGCTTGGAGGAGG	ACCACTGTTGTCCTTGGATTT	qPCR
Human	HDAC-3	ATGACGGTGTCCTTCCACA	TCATAGGTCAGGAGGTCTGCA	qPCR
Human	HDAC-4	TGGAGCTGCTGAATCCTGC	TCATCTTTGGCGTCGTACAT	qPCR
Human	HDAC-5	AACCATCCTCCTTGGAAATCCTG	TCCTTTGACTTCGACAAGAGG	qPCR
Human	HDAC-6	AACCAGGCAGCGAAGAAGTA	ATAAGACTGTGCTGGGCGTGA	qPCR
Human	HDAC-7	TGCTCCTCTACGGCACCAA	TACCTCATCCACAGCCCCACT	qPCR
Human	HDAC-8	AGTCGCTGGTCCCGGTTTA	TGAATGCGTCTTCTACACCAT	qPCR
Mouse	IL-17	AAGGCAGCAGCGATCATCC	GGAACGGTTGAGGTAGTCTGA	qPCR
Mouse	IL-4	AGATGGATGTGCCAAACGTCCTCA	AATATGCGAAGCACCTTGGAAGCC	qPCR
Mouse	IFN-γ	GGCCATCAGCAACAACATAAGCGT	TGGGTTGTTGACCTCAAACTTGGC	qPCR
Mouse	IL-23	ATGCTGGATTGCAGAGCAGTA	ACGGGGCACATTATTTTTAGTCT	qPCR
Mouse	IL-10	GCTCTTACTGACTGGCATGAG	CGCAGCTCTAGGAGCATGTG	qPCR
Human	IL-17-P1	CTCTGACAAGACAACTTTTATCT	CATTTCCTAGTCAATGACATCTG	ChIP
Human	IL-17-P2	TGTCTGTTGCTGAGTAACTTGAG	AAGCAAATTGATTAGTACATGATGA	ChIP
Human	IL-17-P3	TGTACTAATCAATTTGCTTATTCATGC	TACAATCATGGTGGAAGGAGAAG	ChIP
Human	IL-17-P4	TGCTTGCTTCCCCTTCTCCTTCC	GGAGCACGTTCCTCACTTGGTTC	ChIP
Human	IL-17-P5	TATCTTGCCCCAAGTCACCCATC	CCTACGGATTTACTGAGCACCCA	ChIP
Human	IL-17-P6	ATGGGTGCTCAGTAAATCCGTAG	CTGCCACTTACTAGCTATGTGAACT	ChIP

Human	IL-17-P7	AAATCAGCACTGTTTACTTGGAG	ATTAGGTTAATCCTGTTCCTTGA	ChIP
Human	IL-17-P8	TAGCCACTAATGTCACCAAATGC	CAAGGCACTGAGATACTCCCTAG	ChIP
Human	IL-17-P9	AGTACAAACATGATCTTATGAAAGCAA	CTGTTCCACCTATGAGCATTTTG	ChIP
Human	IL-17-P10	TCATAGGTGGAACAGCAGGAAGC	CTCACCCTCGTTGTGCTAGTTCG	ChIP
Human	IFN-γ-P1	CTCTGACAAGACAACTTTTATCT	CTCTGACAAGACAACTTTTATCT	ChIP
Human	IFN-γ-P2	TGTCTGTTGCTGAGTAACTTGAG	AAGCAAATTGATTAGTACATGATGA	ChIP
Human	IFN-γ-P3	TGTACTAATCAATTTGCTTATTCATGC	TACAATCATGGTGGAAGGAGAAG	ChIP
Human	IFN-γ-P4	TGCTTGCTTCCCCTTCTCCTTCC	GGAGCACGTTCCTCACTTGGTTC	ChIP
Human	IFN-γ-P5	TATCTTGCCCCAAGTCACCCATC	CCTACGGATTTACTGAGCACCCA	ChIP
Human	IFN-γ-P6	ATGGGTGCTCAGTAAATCCGTAG	CTGCCACTTACTAGCTATGTGAACT	ChIP
Human	IFN-γ-P7	AAATCAGCACTGTTTACTTGGAG	ATTAGGTTAATCCTGTTCCTTGA	ChIP
Human	IFN-γ-P8	TAGCCACTAATGTCACCAAATGC	CAAGGCACTGAGATACTCCCTAG	ChIP
Human	IFN-γ-P9	AGTACAAACATGATCTTATGAAAGCAA	CTGTTCCACCTATGAGCATTTTG	ChIP
Human	IFN-γ-P10	TCATAGGTGGAACAGCAGGAAGC	CTCACCCTCGTTGTGCTAGTTCG	ChIP

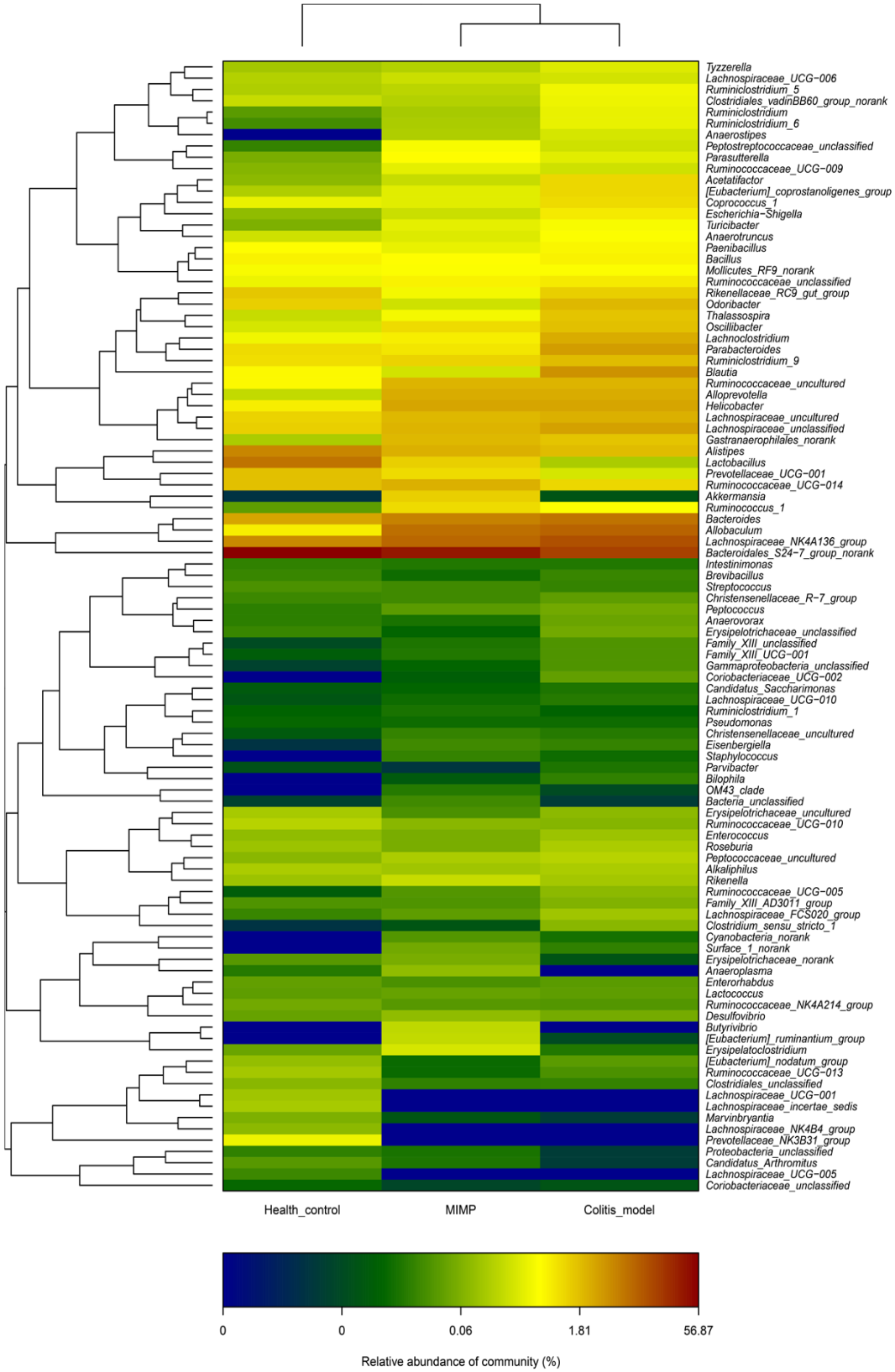

Supplementary Figure S1： The heatmap provides an overview of the bacterial community abundance at the genus level in the healthy control, MIMP group and DSS group.

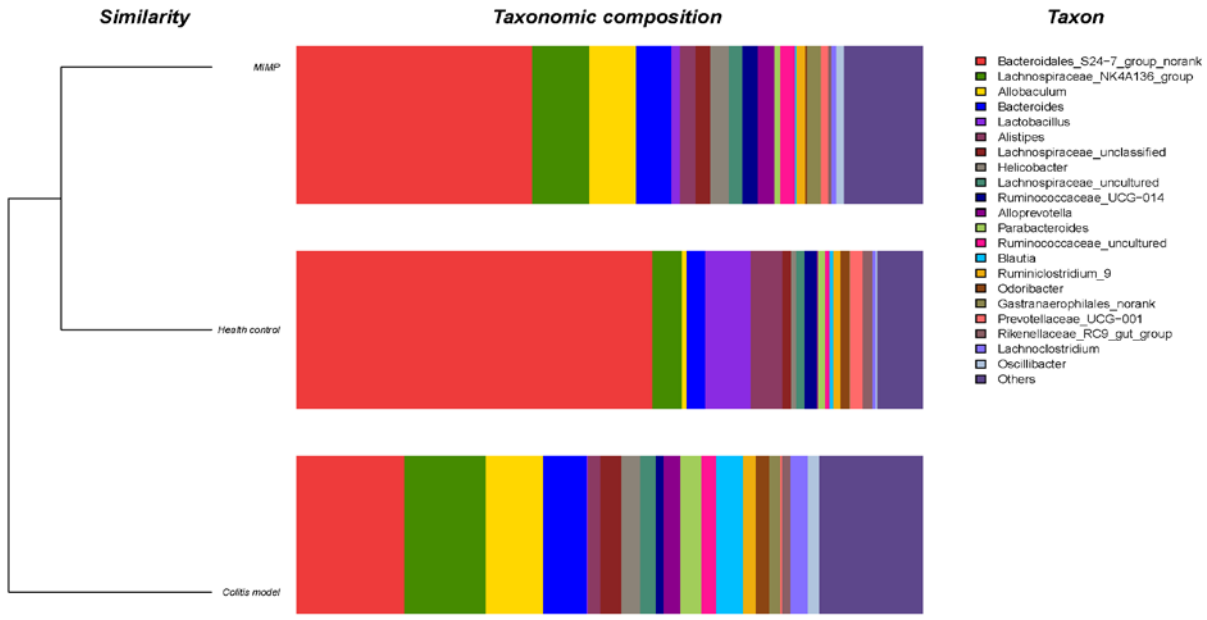

Supplementary Figure S2： Hierarchical cluster analysis shows the structures of the bacterial communities at the genus level in health control, MIMP group and DSS treatment group. Health control and MIMP have a similar bacterial distribution, in which Bacteroidales_S24-7 was particularly enriched in both groups (56.84 and 37.65% respectively).

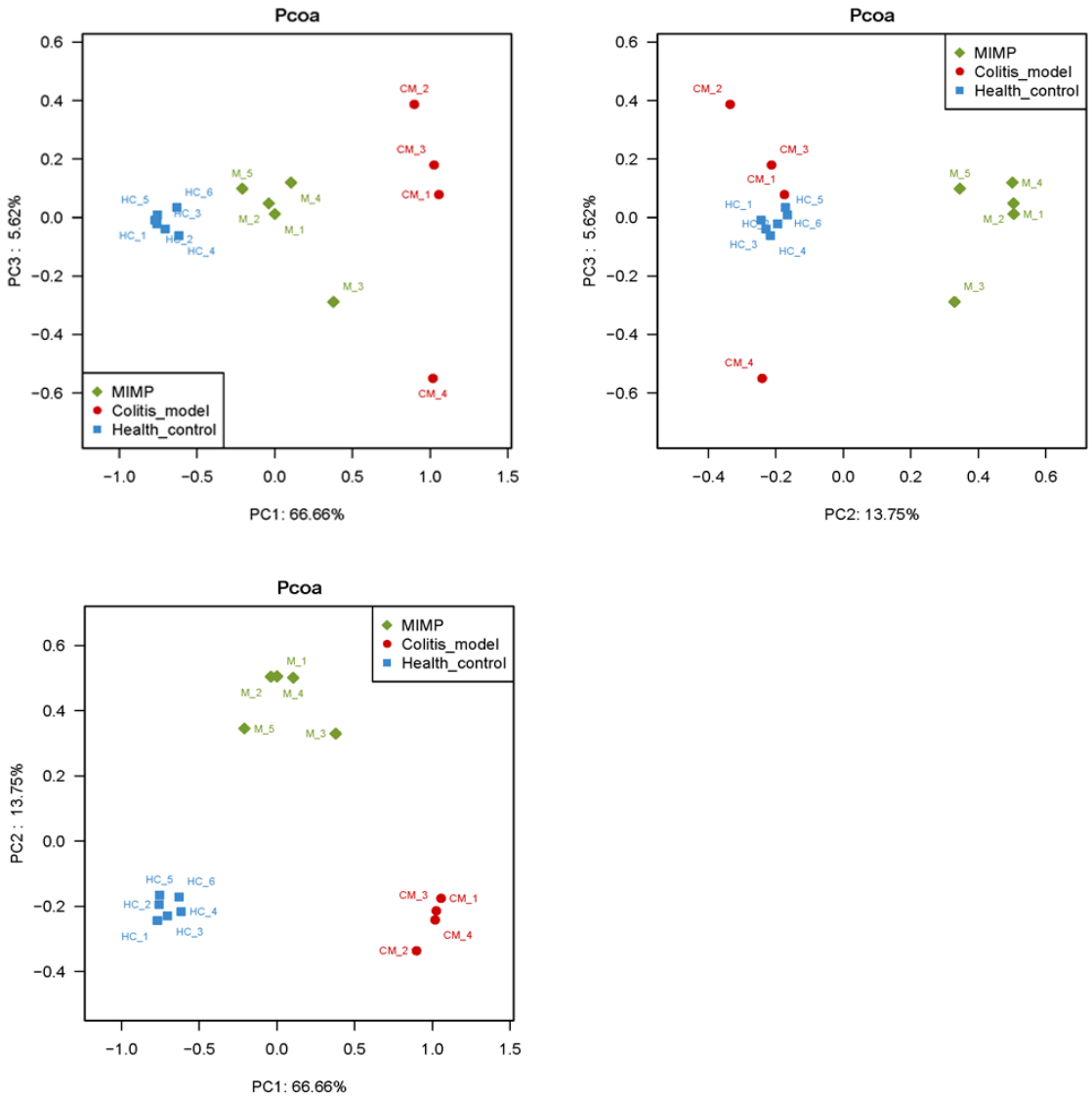

Supplementary Figure S3： The PCoA analysis based on the top three principal components (PC1, PC2 and PC3) reveals that the microbiota compositions of the three groups were completely distinguished by PC1 (66.66%) and PC2 (13.75%). MIMP groups showed more similar microbiota composition of health control than DSS treatment group, as distinguished by PC1 (66.66%) and PC3 (5.62%).

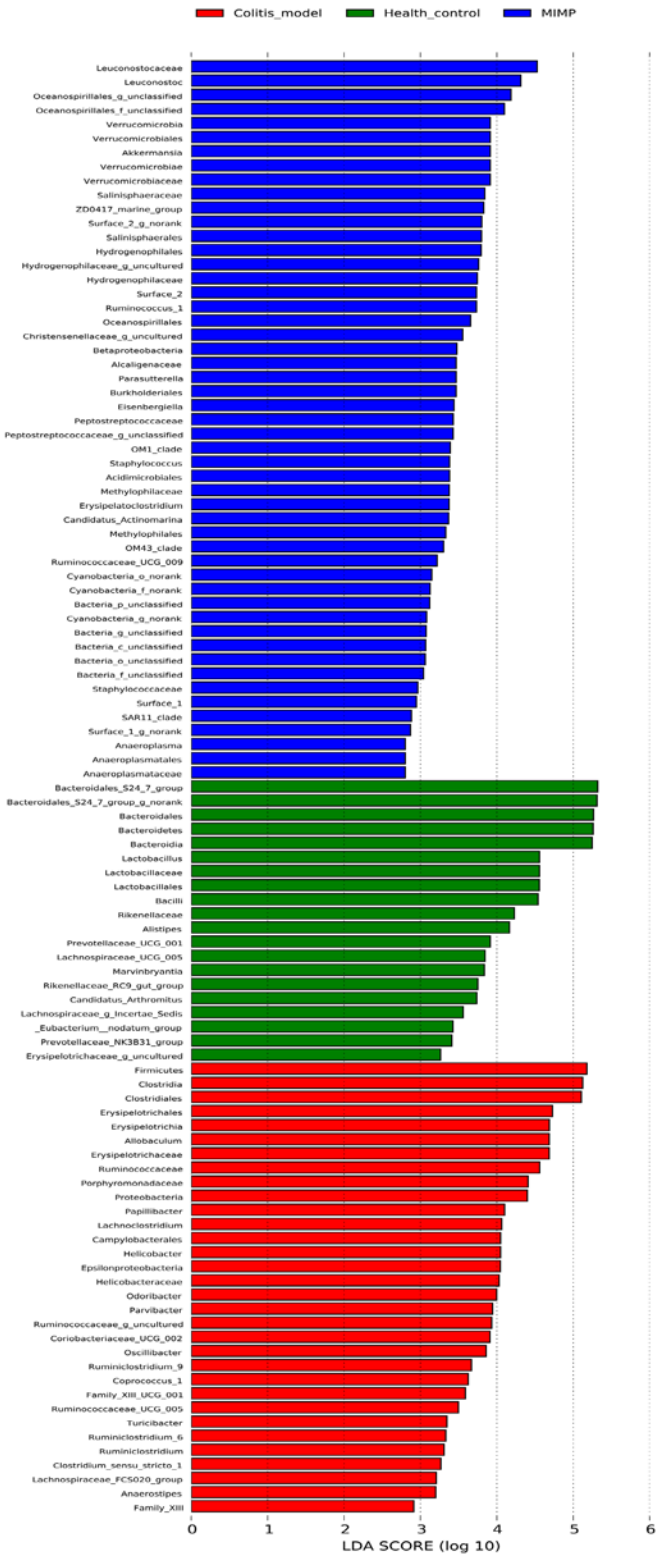

Supplementary Figure S4： The histogram for differentially abundant gut microbiota in three group was constructed based on Lefse analysis. Firmicute and clostridia were enriched in the DSS-treatment group, while Leuconostocaceae and Leuconostoc were abundant in the MIMP group and Bacteroidales_S24-7 and Bacteroidales in the healthy control group.

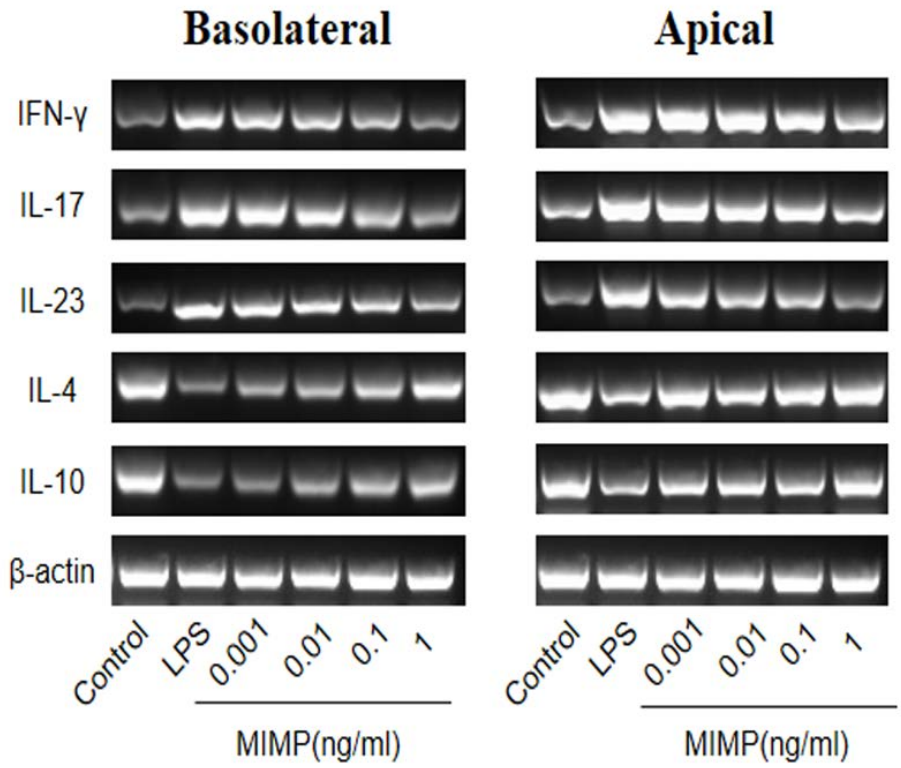

Supplementary Figure S5： After LPS induction, the semi-quantitative RT-PCR shows that MIMP regulates the mRNA level of IL-10, IL-4, IL-17, IL-23 and IFN-γ in the cell-free supernatants from the basolateral chamber(left) and apical chamber(right) at a dose-dependent manner, with an optimal concentration of 1ng/ml. β-actin serves as an internal control.

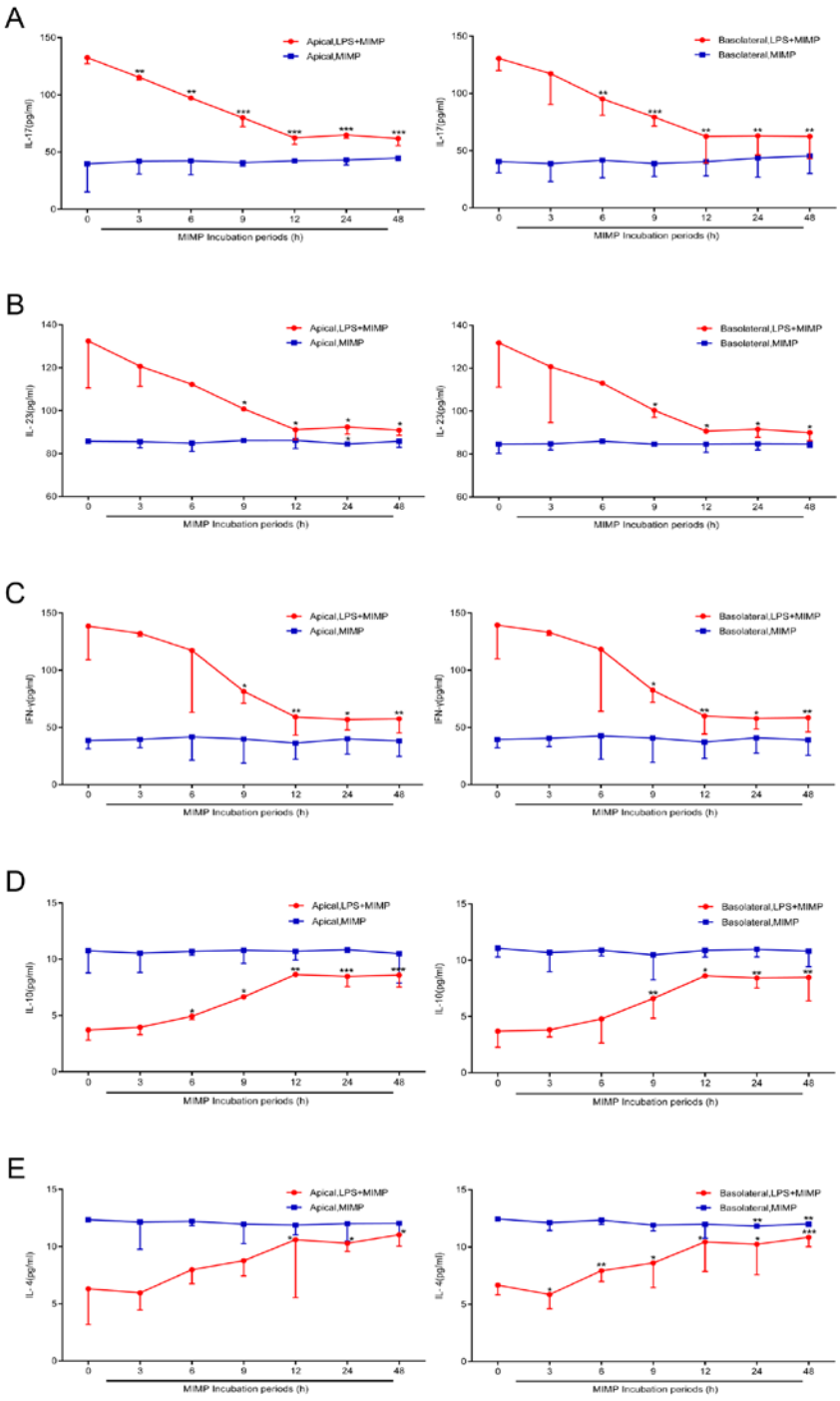

Supplementary Figure S6： After LPS induction, MIMP treatment (1ng/ml) inhibits the secretion of pro-inflammatory IL-17 (A), IL-23 (B) and IFN-γ (C), promotes the secretion of anti-inflammatory IL-4 (D), IL-10 (E) in the cell free supernatants of the basolateral (left)and apical (right) compartment at a time-dependent manner, with an optimal intervening time of 12h. Data are expressed as mean ± SD (*P<0.05, **P<0.01,***P<0.001)

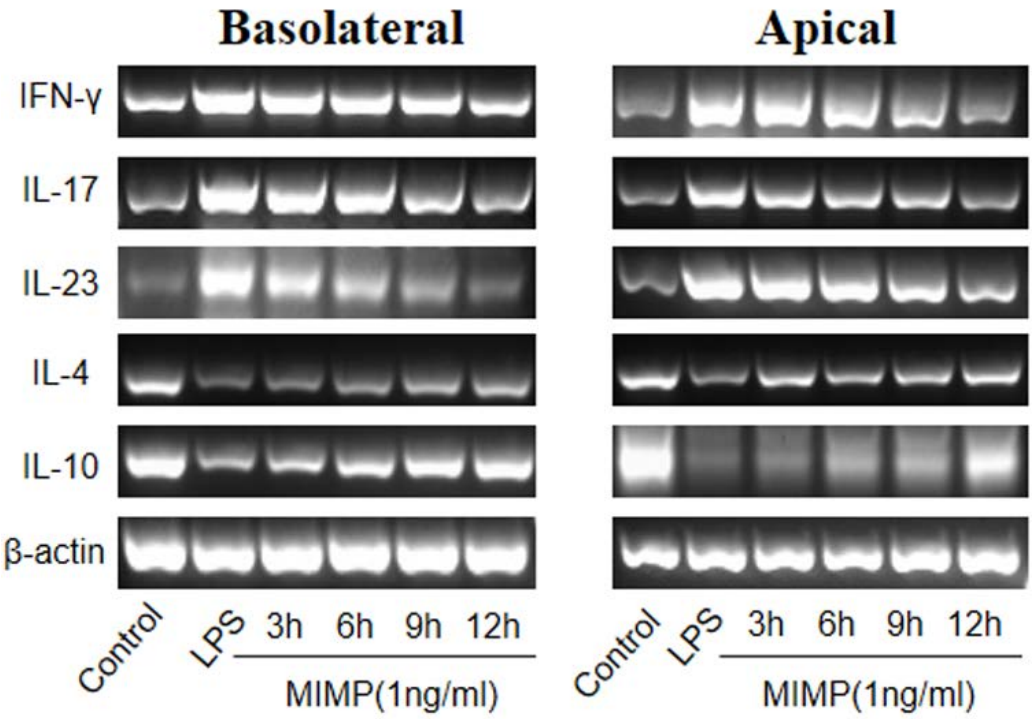

Supplementary Figure S7： After LPS induction, the semi-quantitative RT-PCR shows that MIMP regulates the mRNA level of IL-10, IL-4, IL-17, IL-23 and IFN-γ in the cell-free supernatants from the basolateral chamber(left) and apical chamber(right) at a time-dependent manner, with an optimal intervening time of 12h. β-actin serves as an internal control.

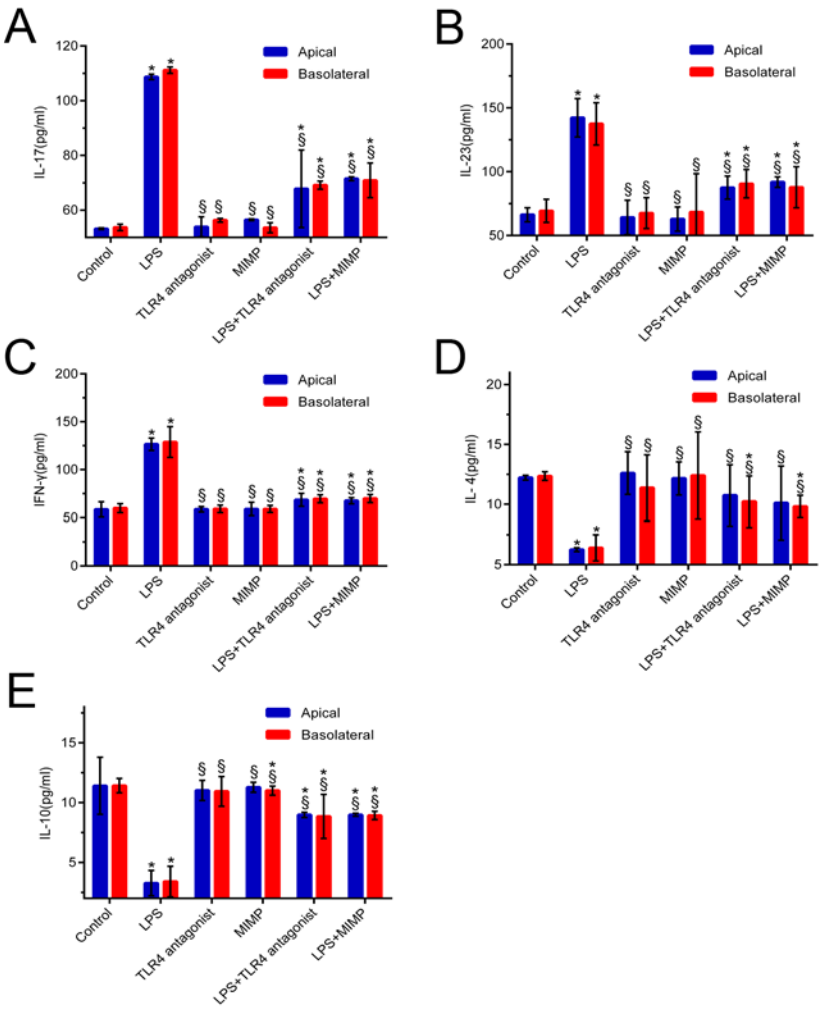

Supplementary Figure S8： TLR4 antagonist, similar to MIMP, suppresses apical and basolateral secretion of IL-17 (A), IL-23 (B) and IFN-γ (C) induced by LPS, and promotes the apical and basolateral secretion of IL-4 (D) and IL-10 (E) inhibited by LPS. Data are expressed as mean ± SD (*P< 0.05 versus control; §P < 0.05 versus LPS-induced cells.).

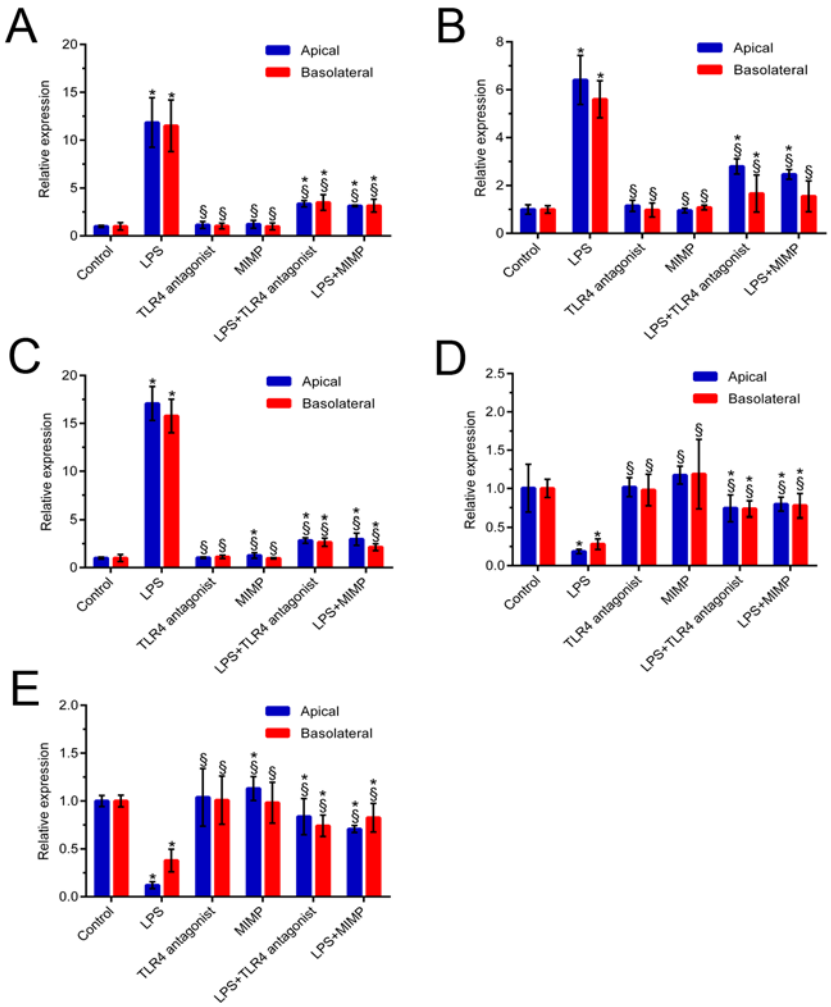

Supplementary Figure S9： After LPS induction, RT-PCR analysis shows TLR4 antagonist and MIMP inhibits the mRNA level of IL-17 (A), IL-23 (B) and IFN-γ (C), promotes the mRNA level of IL-4 (D) and IL-10 (E) in the cell-free supernatants from the apical chamber and basolateral chamber. Data are expressed as mean ± SD (*P < 0.05 versus control; §P < 0.05 versus LPS-induced cells.).

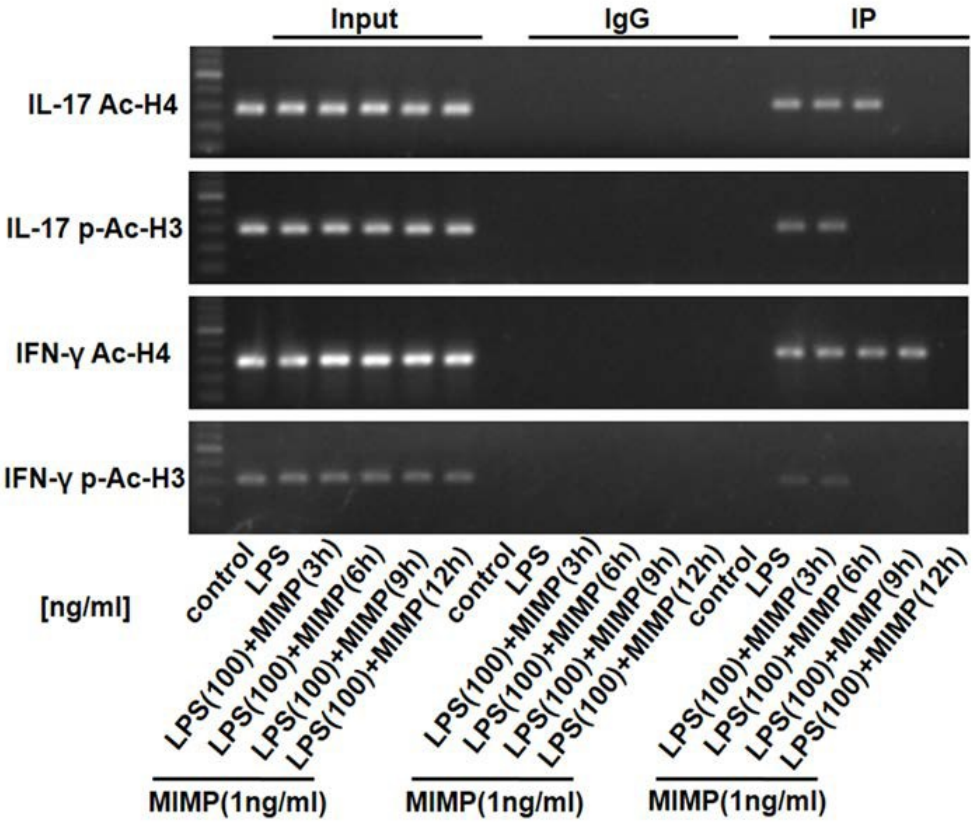

Supplementary Figure S10 : The chromatin immunoprecipitation assay demonstrates that MMIP decreases the LPS-induced binding of phosphoacetylated histone H3 (p-Ser-10/Ac-Lys-14-H3) or acetylated H4 (anti-acetyl-histone-H4) to the IL-17 and IFN- γ promoter at a time-dependent manner, with an optimal intervening time of 12h. PCR products were separated by agarose gel electrophoresis and detected by ethidium bromide staining. PCR amplifications of the IL-17 and IFN-γ promoter of the total DNA was used as positive control (input), IgG was used as negative control.

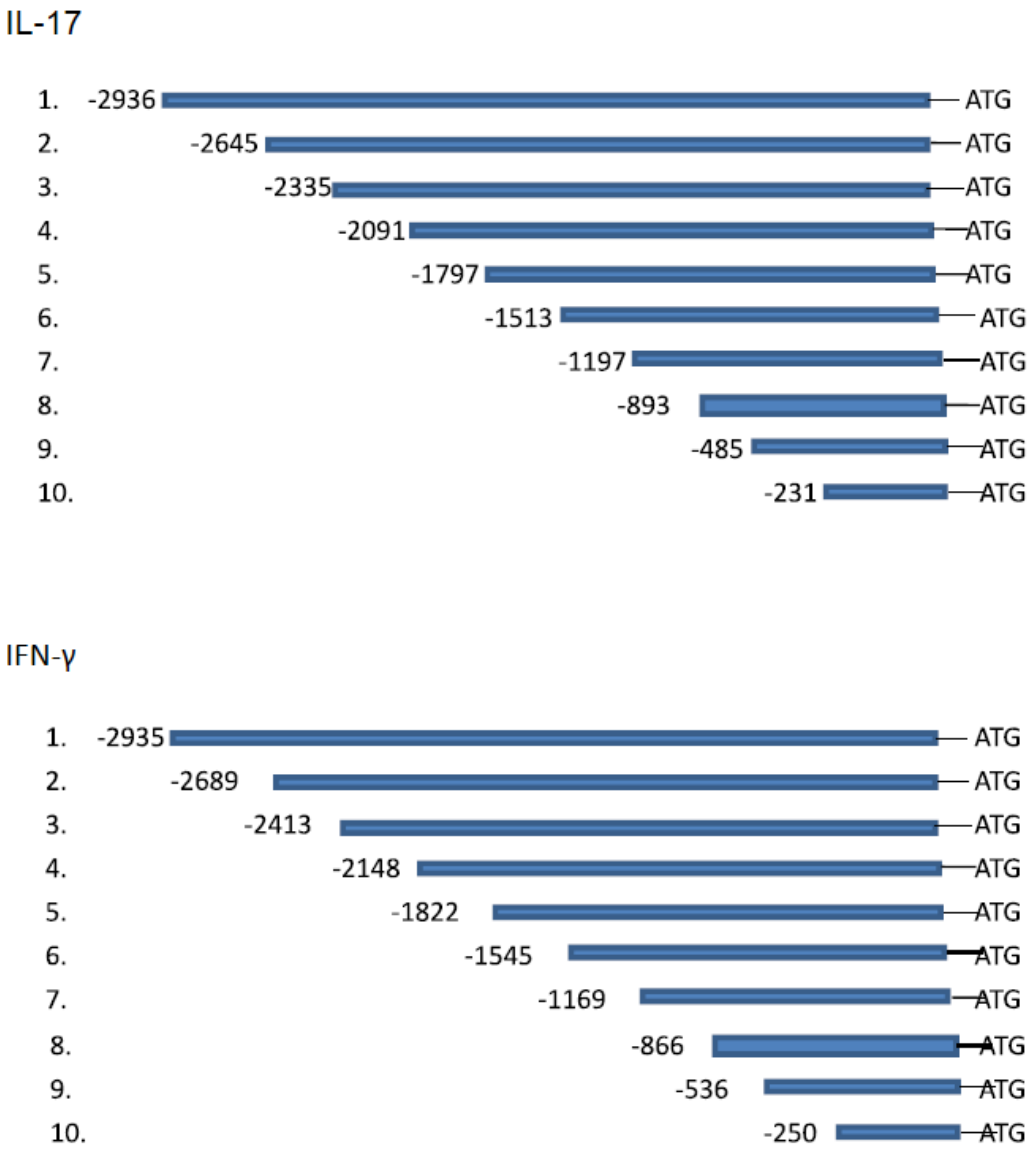

Supplementary Figure S11： The diagrams for the promoter region of IL-17 (upper panel) and IFN-γ (bottom panel) used for constructing the reporter plasmids.